

Design of a fixed-order RST controller for interval systems: application to the control of piezoelectric actuators

Sofiane Khadraoui, Micky Rakotondrabe and Philippe Lutz

ABSTRACT

This paper presents a technique to design a robust polynomial *RST* controller for parametric uncertain systems. The uncertain parameters are assumed to be bounded by intervals. The computation of the controller is addressed by introducing the interval arithmetic. The controller synthesis is formulated as a set inversion problem that can be solved using the SIVIA algorithm. The proposed method is afterwards applied to design a robust controller for a piezoelectric microactuator. The experimental results show the efficiency of the proposed method. Finally, a fine stability analysis is performed to analytically prove the robustness of the designed controller.

Key Words: Parametric uncertainty, interval model, robust performance, RST controller design, piezoelectric microactuators.

I. Introduction

During the last decade, the problem of designing robust control laws for parametric uncertain systems has attracted much attention [1, 2, 3, 4, 5, 6, 7, 8, 9]. Practical considerations have motivated the study of control systems with unknown but bounded parameters uncertainties. Indeed, these uncertainties are often due to various factors such as the sensitivity to the environment conditions (vibrations, evolution of ambient temperature, etc), nonlinearities (hysteresis, time varying parameters, creep, etc), sensors limitation and un-modelled dynamics of systems [1, 5, 6]. If not considered, these uncertainties cause the degradation of the closed-loop performances or the loss of stability. It is therefore necessary to take them into account and to incorporate enough robustness to the controller in order to maintain the nominal performances.

The compensation of these parametric uncertainties is often accomplished by means of adaptative control [9, 10] or by means of robust control laws such as H_2 , H_∞ and μ -synthesis [11, 12]. The adaptative control methods require a precise model which is difficult to obtain. Concerning the robust H_2 , H_∞ and μ -synthesis approaches, their efficiency is proved in several applications (SISO and MIMO systems) while their major disadvantage is the derivation of high-order controllers which are time consuming and which limit their embedding possibilities, particularly for embedded microsystems. One way to represent parametric uncertainties is to let each parameter takes its value within a range called interval [3, 4, 13]. In addition to the natural way and simplicity of using intervals to bound uncertain parameters, interval arithmetic presents a symbolic or a numeric certificate to the results. Thus, using interval arithmetic to modeling and control design leads to certified robust stability and performances if a solution exists. For instance, the stability analysis of a characteristic polynomial subjected to uncertain parameters has been discussed in many works [3, 14, 15]. It was often based on the Routh's criteria and/or on the Kharitonov's theorem. The

Manuscript received April, 2011. This work is supported by the Conseil General du Doubs.

FEMTO-ST Institute, UMR CNRS 6174-UFC/ENSMM/UTBM, Automatic Control and Micro-Mechatronic Systems depart., AS2M, 24 rue Alain Savary, Besançon 25000, France. Corresponding author: mrakoton@femto-st.fr

work in [16] presents the stability of uncertain systems with interval time-varying delay. [17] discusses an approach to design robust stabilizing controller for interval systems in the state-space representation. A systematic computational technique to design robust stabilizing controller for interval systems using constrained optimization problem was proposed in [18]. While the above works consider robust stability, robustness on performances for interval systems has also been discussed in several work [19, 4, 20, 21, 22, 23]. The work in [19] presents an interesting result on the inclusion of interval systems performances. [20] proposed a prediction-based control algorithm and its application to a welding process modelled by intervals. In [21], a state feedback controller was first considered to ensure the robust stability, then a pre-filter that guarantees the required performances was constructed by applying a curve fitting technique. In [22], an approach to design a robust PID controller for interval transfer function was derived. However the method was limited to 2^{nd} order uncertain systems. In the previous work [23], we proposed to extend the method for n^{th} order uncertain systems but still with zero-order numerator. However, the order of the derived controller was not *a priori* fixed and thus might not adapted to the hardware for implementation in embedded microsystems.

In this paper, we propose the interval modeling of a generalized n^{th} order uncertain parameters (without restriction on the numerator's order), and the design of a robust fixed-order controller to ensure specified performances. The robust controller considered in this contribution is a polynomial *RST* controller. The polynomials *R* and *S* allow to create a feedback control in order to be robust to the uncertainties, while the polynomial *T* is introduced in the feedforward to improve the tracking. The computation of these polynomials is based on the inclusion performances theorem [19]. The main advantages of the proposed method relative to existing works are: 1) no restriction is imposed on the system order, 2) and the order of the controller is *a priori* fixed and thus low-order (robust) controllers can be yielded. Furthermore, the suggested approach in this paper is simple and involves less computational complexity. The controller synthesis problem is formulated as a set-inversion problem defined as the inclusion parameter by parameter.

The paper is organized as follows. In section-II, preliminaries related to interval arithmetic and

systems are reminded. Section-III is dedicated to the computation of the controller using the proposed approach. In section-IV, we apply the proposed method to model and control piezoelectric actuators. The experimental results and discussion are presented in section-V. Finally, to evaluate the robustness of the implemented controller, a closed-loop stability analysis is presented in section-VI.

II. Interval analysis preliminaries

2.1. Definition of interval

An interval $[x]$ can be defined by the set of all real numbers given as follows:

$$[x] = [x^-, x^+] = \{x \in \mathbb{R} / x^- \leq x \leq x^+\} \quad (1)$$

x^- and x^+ are the left and right endpoints respectively. $[x]$ is degenerate if $x^- = x^+$.

The width of an interval $[x]$ is given by:

$$width([x]) = x^+ - x^- \quad (2)$$

The midpoint of $[x]$ is given by:

$$mid([x]) = \frac{x^+ + x^-}{2} \quad (3)$$

The radius of $[x]$ is defined by:

$$rad([x]) = \frac{x^+ - x^-}{2} \quad (4)$$

2.2. Operations on intervals

The result of an operation between two intervals is an interval that contains all possible solution as follows. Given two intervals $[x] = [x^-, x^+]$, $[y] = [y^-, y^+]$ and $\circ \in \{+, -, \cdot, /\}$, we can write:

$$[x] \circ [y] = \{x \circ y \mid x \in [x], y \in [y]\} \quad (5)$$

Therefore, the sum of two intervals $[x] + [y]$ is given by:

$$[x] + [y] = [x^- + y^-, x^+ + y^+] \quad (6)$$

the difference of two intervals $[x] - [y]$ is:

$$[x] - [y] = [x^- - y^+, x^+ - y^-] \quad (7)$$

the product of two intervals $[x] \cdot [y]$ is:

$$[x] \cdot [y] = [\min(x^-y^-, x^-y^+, x^+y^-, x^+y^+), \max(x^-y^-, x^-y^+, x^+y^-, x^+y^+)] \quad (8)$$

and finally, the quotient $[x]/[y]$ is given by

$$[x]/[y] = [x] \cdot [1/y^+, 1/y^-], 0 \notin [y] \quad (9)$$

The intersection of two intervals $[x] \cap [y]$ is defined by:

1- if $y^+ < x^-$ or $x^+ < y^-$ the intersection is an empty set:

$$[x] \cap [y] = \emptyset \quad (10)$$

2- Otherwise:

$$[x] \cap [y] = [\max\{x^-, y^-\}, \min\{x^+, y^+\}] \quad (11)$$

In the latter case, the union of $[x]$ and $[y]$ is also an interval:

$$[x] \cup [y] = [\min\{x^-, y^-\}, \max\{x^+, y^+\}] \quad (12)$$

When $[x] \cap [y] = \emptyset$, the union of the two intervals is not an interval. For that, the interval hull is defined:

$$[x] \sqcup [y] = [\min\{x^-, y^-\}, \max\{x^+, y^+\}] \quad (13)$$

it is verified that: $[x] \cup [y] \subseteq [x] \sqcup [y]$ for any two intervals $[x]$ and $[y]$.

2.3. Interval systems

Definition II.1 *Parametric uncertain systems can be modelled by interval systems. A SISO interval system that defines a family of systems is denoted $[G](s, [p], [q])$ and is given by:*

$$\begin{aligned} [G](s, [p], [q]) &= \frac{\sum_{j=0}^m [q_j] s^j}{\sum_{i=0}^n [p_i] s^i} \\ &= \left\{ \frac{\sum_{j=0}^m p_j s^j}{\sum_{i=0}^n p_i s^i} \mid p_i \in [p_i^-, p_i^+], p_j \in [p_j^-, p_j^+] \right\} \end{aligned} \quad (14)$$

Such as: $[q] = [[q_0], \dots, [q_m]]$ and $[p] = [[p_0], \dots, [p_n]]$ are boxes (i.e. vectors of interval).

The following lemma and theorem concern the performances of two interval systems and are due to [19]. Consider two interval systems having the same structure (degrees of polynomials):

$$[G_1](s) = \frac{\sum_{j=0}^m [b_{1j}] s^j}{\sum_{i=0}^n [a_{1i}] s^i} \quad (15)$$

and

$$[G_2](s) = \frac{\sum_{l=0}^m [b_{2l}] \cdot s^l}{\sum_{k=0}^n [a_{2k}] \cdot s^k} \quad (16)$$

Lemma II.1 *(Inclusion of two interval systems)*

$$\text{if } \begin{cases} [a_{1k}] \subseteq [a_{2k}], \quad \forall k = 1 \dots n \\ \text{and} \\ [b_{1l}] \subseteq [b_{2l}], \quad \forall l = 1 \dots m \end{cases}$$

$$\Rightarrow [G_1](s) \subseteq [G_2](s);$$

Theorem II.1 *(Performances inclusion theorem)*

$$\text{if } [G_1](s) \subseteq [G_2](s);$$

$$\Rightarrow \begin{cases} [g_1](t) \subseteq [g_2](t) \quad \forall t \\ \begin{cases} [\rho]([G_1](j\omega)) \subseteq [\rho]([G_2](j\omega)) \\ [\varphi]([G_1](j\omega)) \subseteq [\varphi]([G_2](j\omega)) \end{cases} \quad \forall \omega \end{cases}$$

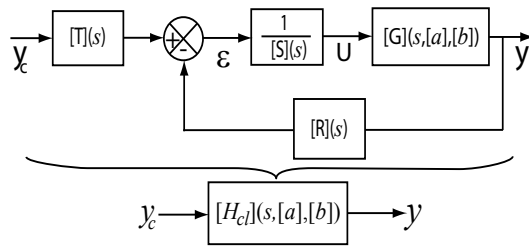
where $[g_i](t)$ is the (temporal) impulse response of system $[G_i](s)$, $[\rho]([G_i](j\omega))$ is its modulus and $[\varphi]([G_i](j\omega))$ is its phase.

Proof II.1 See [19].

Theorem II.1 states that if $[G_1](s)$ is included in $[G_2](s)$, its temporal response (impulse response, step response, etc.) will be included in that of $[G_2](s)$. The same holds for the frequential response (bode, nyquist, black-nichols). Such inclusion of responses directly induces the performances inclusion and can be used to design a robust controller as we propose in this paper.

III. Problem statement

Consider an interval system $[G](s, [a], [b])$ to be controlled by a RST controller (Fig. 1). The choice of the RST structure of controller is that it is a more general structure. The PID controller is a particular case of the RST controller when $R(s) = T(s)$. Now, the problem consists in finding the different polynomials R , S and T of the controller that ensures some given performances for the closed-loop $[H_{cl}](s, [a], [b])$ (see Fig. 1) whatever the parameters a and b ranging in $[a]$ and $[b]$ respectively.

Fig. 1. Closed-loop transfer $[H_{cl}](s, [a], [b])$.

In the sequel, the system $[G](s, [a], [b])$ will be denoted by:

$$[G](s, [a], [b]) = \frac{[N](s, [b])}{[D](s, [a])} \quad (17)$$

where $[N](s, [b])$ and $[D](s, [a])$ are interval polynomials defined by:

$$[N](s, [b]) = 1 + \sum_{j=1}^m [b_j] s^j$$

$$[D](s, [a]) = \sum_{i=0}^n [a_i] s^i$$

Such as $[a] = [[a_0], \dots, [a_n]]$, $[b] = [1, [b_1], \dots, [b_m]]$ and $m \leq n$.

This form of representation (unit on the numerator) facilitates the application of the proposed control method. In fact, it is always possible to describe the system using this representation form.

Consider the following performances that we expect for the closed-loop:

- no overshoot.
- settling time $tr_{5\%} \in [tr^-, tr^+]$.
- static error $|\varepsilon| \leq \eta$

These specifications can be easily described by means of an interval model called interval reference model denoted $[H](s)$:

$$[H](s) = \frac{[K_e]}{1 + [\tau]s} \quad (18)$$

where $[\tau] = [\tau^-, \tau^+]$, $[K_e] = [K_e^-, K_e^+]$.

Settling time and static error of (18) are defined by $[tr_{5\%}] = 3 \cdot [\tau]$ and $|\varepsilon| = |[K_e] - 1|$ respectively.

Based on [Theorem II.1](#), the following problem is therefore addressed.

Problem III.1 Given an interval system $[G](s)$ and an interval reference model $[H](s)$ that defines some given performances, find a controller $[C](s)$ such that $[H_{cl}](s) \subseteq [H](s)$. In other words, the problem consists in finding a set of controllers $C(s)$, gathered in an interval $[C](s)$, such that the performances of the closed-loop $[H_{cl}](s)$ are included in the specified performances.

3.1. Computation of the closed-loop model $[H_{cl}](s)$

In this part, we compute the closed-loop model using the interval system and the controller transfers. The generalized form of the *RST* controller can be defined as follows:

$$[R](s) = \sum_{i=1}^{r_n} [r_i] s^i$$

$$[S](s) = \sum_{i=1}^{s_n} [s_i] s^i \quad (19)$$

$$[T](s) = \sum_{i=1}^{t_n} [t_i] s^i$$

such as $s_n \geq r_n \geq t_n$ in order to have the causality of the controller.

Let us now define fixed-order *RST* structure with a fixed and low degree for each interval polynomials $[R]$, $[S]$ and $[T]$. Polynomials with first-degree are chosen for that:

$$[R](s) = [r_1]s + [r_0]$$

$$[S](s) = [s_1]s + [s_0] \quad (20)$$

$$[T](s) = [t_1]s + 1$$

We have chosen t_0 equals to one in order to minimize the number of the controller parameters to be sought for. On the one hand, this facilitates the computation of the controller. On the other hand, even if we choose $t_0 \neq 1$, any setting on the parameters t_1 , r_1 and r_0 will lead to $t_0 = 1$.

Remark III.1 If further we cannot find a controller $[C](s)$ that satisfies [Problem III.1](#), the degree of one or more of the polynomials $[R]$, $[S]$ and $[T]$ can be increased and the controller synthesis is performed again.

Let us define the box of the controller parameters $[\theta] = [[t_1], [r_1], [r_0], [s_1], [s_0]]$.

From [Fig. 1](#), and using the interval system (17) and the controller *RST* (20), the interval closed-loop transfer $[H_{cl}](s, [a], [b], [\theta])$ is derived:

$$[H_{cl}](s, [a], [b], [\theta]) = \frac{[T](s)}{\frac{[S](s)}{[G](s, [a], [b])} + [R](s)} \quad (21)$$

(21) can be rewritten as follows:

$$[H_{cl}](s, [a], [b], [\theta]) = \frac{[T](s) \cdot [N](s, [b])}{[S](s) \cdot [D](s, [a]) + [R](s) \cdot [N](s, [b])} \quad (22)$$

After replacing the different polynomials, we obtain the interval closed-loop transfer $[H_{cl}](s, [a], [b], [\theta])$ depending on the different interval parameters:

$$[H_{cl}](s, [a], [b], [\theta]) = \frac{([t_1]s+1)(1+\sum_{j=1}^m [b_j]s^j)}{([s_1]s+[s_0])\sum_{i=0}^n [a_i]s^i + ([r_1]s+[r_0])(1+\sum_{j=1}^m [b_j]s^j)} \quad (23)$$

After developing (23), we obtain:

$$[H_{cl}](s, [p], [q]) = \frac{1 + \sum_{j=1}^e [q_j]s^j}{\sum_{i=0}^r [p_i]s^i} \quad (24)$$

Where $e = m + 1$ and $r = n + 1$. The boxes of interval parameters $[p]$ and $[q]$ are function of the boxes $[a]$, $[b]$ and $[\theta]$.

3.2. Controller derivation

The main objective consists to find the set Θ of the controller parameters vector for which robust performances hold:

$$\Theta := \{\theta \in [\theta] \mid [H_{cl}](s, [p], [q]) \subseteq [H](s)\} \quad (25)$$

This computation of Θ is feasible if and only if $[H_{cl}](s, [p], [q])$ has the same structure than $[H](s)$, i.e. their numerators have the same degree and the same holds for their denominators. As the structure of $[H_{cl}](s, [p], [q])$ is *a priori* fixed, we should adjust the structure of $[H](s)$ to satisfy such condition if it was not yet the case. For that, first let us have a look on the structure of $[H_{cl}](s, [p], [q])$ as in (24). The degree of the numerator is $(m + 1)$ while it is $(n + 1)$ for the denominator. Let us now adjust the structure of $[H](s)$ (see (18)) in order to have the same structure by adding some zeros and poles far away from the imaginary axe. This leads to the following reference model:

$$[H](s) = \frac{(1 + \frac{[\tau]}{\kappa}s)^{m+1}}{\frac{1}{[K_e]} \cdot (1 + [\tau]s)(1 + \frac{[\tau]}{\kappa}s)^n} \quad (26)$$

With $\kappa \gg 1$.

After developing (26), we have:

$$[H](s, [w], [x]) = \frac{1 + \sum_{j=1}^{m+1} [x_j]s^j}{\sum_{i=0}^{n+1} [w_i]s^i} \quad (27)$$

Where $[x_j]$ and $[w_i]$ (for $j = 1, \dots, m + 1$ and $i = 0, \dots, n + 1$) are functions of the interval parameters $[K_e]$, $[\tau]$ and of the real number κ .

3.3. Inclusion condition

The research of parameter Θ in (25) of the controller is done by using the inclusion $[H_{cl}](s) \subseteq [H](s)$ (see Problem III.1). However, according to Lemma II.1, such inclusion can be satisfied by considering the inclusion of each parameter of $[H_{cl}](s)$ inside that of $[H](s)$. Thus, by using (24) and (27), the problem becomes the research of the controller parameters under the following constraints:

$$\begin{aligned} [q_j] &\subseteq [x_j], \forall j = 1, \dots, m + 1 \\ [p_i] &\subseteq [w_i], \forall i = 0, \dots, n + 1 \end{aligned} \quad (28)$$

and therefore, the computation problem in (25) of the set parameters Θ is reduced to the following problem:

$$\Theta := \left\{ \theta \in [\theta] \mid \begin{aligned} [q_j](\theta) &\subseteq [x_j], \forall j = 1, \dots, m + 1 \\ [p_i](\theta) &\subseteq [w_i], \forall i = 0, \dots, n + 1 \end{aligned} \right\} \quad (29)$$

This problem is known as a *Set-Inversion Problem* which can be solved using interval techniques [3, 13]. The set inversion operation consists to compute the reciprocal image of a compact set called subpaving. The set-inversion algorithm SIVIA (more details are given in [3, 24]) allows to approximate with subpavings the set solution Θ described in (29). This approximation is realized with an inner and outer subpavings, respectively $\underline{\Theta}$ and $\bar{\Theta}$, such that $\underline{\Theta} \subseteq \Theta \subseteq \bar{\Theta}$. The subpaving $\underline{\Theta}$ corresponds to the controller parameter vector for which the problem (29) holds. If $\bar{\Theta} = \emptyset$, then it is guaranteed that no solution exists for (29).

Tab. 1 resumes the recursive SIVIA algorithm allowing to solve a set inversion problem in intervals. We give in Fig. 2 a flow chart that describes this recursive SIVIA algorithm when applied to the computation of the RST controller parameters and which is given by the problem (29). SIVIA algorithm requires a search box $[\theta_0]$ (possibly very large) called initial box to which $\bar{\Theta}$ is guaranteed to belong. The inner and outer subpavings ($\underline{\Theta}$ and $\bar{\Theta}$) are initially empty.

Table 1. Algorithm SIVIA for solving a set-inversion problem [3, 24].

	SIVIA(in: $[p], [q], [w], [x], [\theta], \epsilon$; inout: $\underline{\Theta}, \bar{\Theta}$)
1	if $[[p]([\theta]), [q]([\theta])] \cap [[w], [x]] = \emptyset$ return;
2	if $[[p]([\theta]), [q]([\theta])] \subseteq [[w], [x]]$ then $\{\underline{\Theta} := \underline{\Theta} \cup [\theta]; \bar{\Theta} := \bar{\Theta} \cup [\theta]\}$ return;
4	if $width([\theta]) < \epsilon$ then $\{\bar{\Theta} := \bar{\Theta} \cup [\theta]\}$; return
5	bisection of $[\theta]$ into $L([\theta])$ and $R([\theta])$;
6	SIVIA($[p], [q], [w], [x], L([\theta]), \epsilon; \underline{\Theta}, \bar{\Theta}$); SIVIA($[p], [q], [w], [x], R([\theta]), \epsilon; \underline{\Theta}, \bar{\Theta}$).

Remark III.2 In the most cases, we are interested to compute an inner subpaving $\underline{\Theta}$ for which we are sure that $\underline{\Theta}$ is included in the set solution Θ , i.e. $\underline{\Theta} \subseteq \Theta$, but when no inner subpaving exists ($\underline{\Theta} = \emptyset$), it is possible to choose parameters inside the outer subpaving, i.e. choose $\theta \in \bar{\Theta}$.

IV. Application to piezocantilevers

In this section, we apply the proposed method to control the deflection of piezoelectric actuators used in microgrippers. The latters are considered as microsystems. These microgrippers are widely used in micromanipulation and microassembly tasks where the required performances are sever (submicrometric accuracy, tens of milliseconds of settling time, no overshoot, etc.) [25]. A microgripper is based on two piezoelectric cantilevers (microactuators) also called piezocantilever [26, 27]. While one piezocantilever is controlled on position (deflection), the second one is controlled on force. This allows to precisely position a manipulated small object by controlling at the same time

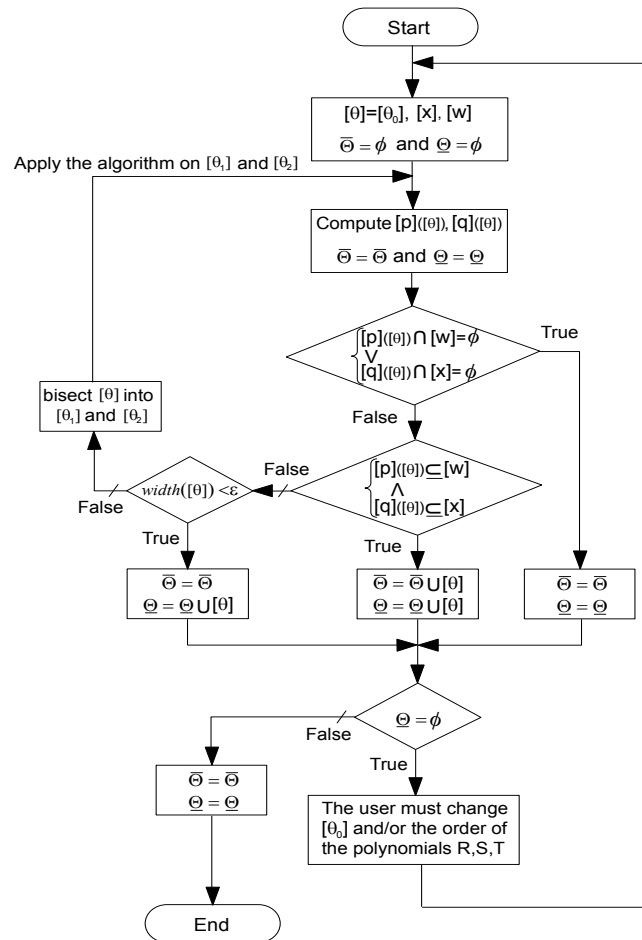


Fig. 2. Algorithm SIVIA used to solve the set-inversion problem (29) [3, 24].

the handling force. In this work, we focus our study on the position control. The piezocantilever used during the experiments is a unimorph piezocantilever with rectangular cross-section. Such cantilever is made up of one piezoelectric layer (piezolayer) and one passive layer. When a voltage U is applied to the piezolayer, it contracts/expands accordingly to the direction of the applied electric field. As the piezolayer and the passive layer are glued themselves, a global deflection y of the structure is yielded (Fig. 3).

Due to their small sizes, piezocantilevers are very sensitive to environment (thermal variation, vibration, surrounding surface forces, etc.) and to the reaction of the manipulated objects. This high sensitivity leads to a change of their behavior during the tasks (manipulation, etc.). Unfortunately, the change of the environment

is hardly known and hardly modelizable at the micro/nano-scale making impossible the use of a kind of real-time adaptive control law. Beyond, this difficulty is confirmed the lack of convenient sensors that can be used to measure the environment variation at this scale. This is why it is more attractive to employ more simplified models and to synthesize robust control laws for piezocantilevers. Classical H_∞ robust control laws have successfully been used in our previous works [28], however the orders of the derived controllers were high and may not be convenient for embedded microsystems such as embedded microgrippers. Controllers that account eventual nonlinearities were also used but they required the use of precise models of these nonlinearities [29, 30] which finally make complex the controller implementation. The technique presented in this paper is thus used. Its advantages are 1) the ease of modeling the parametric uncertainties by just bounding them with intervals, 2) and the derivation of a low order controller since its structure is *a priori* fixed.

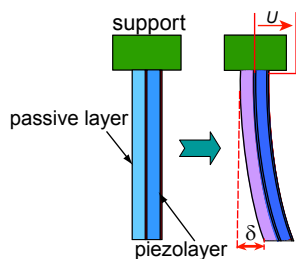


Fig. 3. Principle of a unimorph piezocantilever.

As it is impossible to characterize the model variation of a given piezocantilever during its functioning and then to derive an interval model $[G](s, [a], [b])$, we use the following procedure.

Two piezocantilevers are randomly taken from a set of stock of piezocantilevers having the same dimensions and the same physical characteristics. Such stock is essential in micromanipulation and microassembly context in order to ensure a quick replacement in case of breakage of actuators. In that case, it is rightfully wished that the same controller is used for the new actuator. However, even if these piezocantilevers are physically and geometrically similar, there are always non negligible differences in their models parameters. These differences on models

parameters are due to small and non-perceptible differences in the sizes of the piezocantilevers (in the order of tens of micrometres) due to the fabrication accuracy. The two different models of the chosen piezocantilevers will be therefore used to derive an interval model $[G](s, [a], [b])$.

4.1. Presentation of the setup

Fig. 4 presents the experimental setup. It is composed of:

- two unimorph piezocantilevers. Each piezocantilever is based on a PZT (lead zirconate titanate) for the piezolayer and on copper for the passive layer. The dimensions of the cantilevers are approximately $L \times b \times h = 15\text{mm} \times 2\text{mm} \times 0.3\text{mm}$, where the thicknesses are 0.2mm and 0.1mm for the PZT and for the Copper respectively,
- an optical sensor (Keyence LC-242) used to measure the deflection of the piezocantilevers. The sensor has 10nm of resolution,
- a computer-DSPACE hardware combined with the Matlab-Simulink software for the implementation of the controller and for data acquisition,
- and a high voltage (HV: $\pm 200\text{V}$) amplifier used to amplify the input voltage from the computer-DSPACE material.

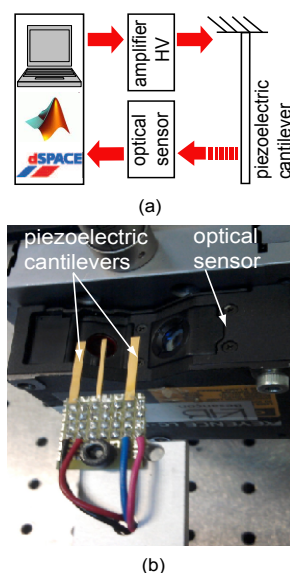


Fig. 4. The experimental setup: piezocantilevers controlled through computer DSpace material.

4.2. Modeling of the two piezocantilevers

The linear relation between the deflection at the tip of the piezocantilever and the applied input voltage U is:

$$\delta = G(s)U \quad (30)$$

To identify the two models $G_1(s)$ and $G_2(s)$ corresponding to the two piezocantilevers, a step response is used. A second order was chosen for the model of each piezocantilever because of its sufficiency to account the first resonance which is sufficient for the expected applications. The identification of the two models $G_1(s)$ and $G_2(s)$ was afterwards performed using output error method and the matlab software. We obtain:

$$G_1(s) = \frac{8.08 \times 10^{-8}s^2 + 1.809 \times 10^{-4}s + 1}{8.753 \times 10^{-8}s^2 + 5.234 \times 10^{-6}s + 1.283}$$

$$G_2(s) = \frac{6.992 \times 10^{-8}s^2 + 1.807 \times 10^{-4}s + 1}{9.844 \times 10^{-8}s^2 + 5.37 \times 10^{-6}s + 1.448} \quad (31)$$

4.3. Derivation of the interval model

Let us rewrite each model $G_i(s)$ ($i = 1, 2$) as follows:

$$G_i(s) = \frac{b_{2i}s^2 + b_{1i}s + 1}{a_{2i}s^2 + a_{1i}s + a_{0i}} \quad (32)$$

The interval model $[G](s, [a], [b])$ which represents a family of piezocantilever models is derived using the two point models $G_i(s)$. Considering each parameter of $G_1(s)$ and its counterpart in $G_2(s)$ as an endpoint of the interval parameter in $[G](s, [a], [b])$, we have:

$$[G](s, [a], [b]) = \frac{[b_2]s^2 + [b_1]s + 1}{[a_2]s^2 + [a_1]s + [a_0]} \quad (33)$$

such as:

$$\begin{aligned} [b_2] &= [\min(b_{21}, b_{22}), \max(b_{21}, b_{22})] \\ [b_1] &= [\min(b_{11}, b_{12}), \max(b_{11}, b_{12})] \\ [a_2] &= [\min(a_{21}, a_{22}), \max(a_{21}, a_{22})] \\ [a_1] &= [\min(a_{11}, a_{12}), \max(a_{11}, a_{12})] \\ [a_0] &= [\min(a_{01}, a_{02}), \max(a_{01}, a_{02})] \end{aligned}$$

After computation, we obtain:

$$\begin{aligned} [b_2] &= [6.992, 8.08] \times 10^{-8} \\ [b_1] &= [1.807, 1.809] \times 10^{-4} \\ [a_2] &= [8.753, 9.844] \times 10^{-8} \\ [a_1] &= [5.234, 5.37] \times 10^{-6} \\ [a_0] &= [1.283, 1.448] \end{aligned}$$

To increase the stability margin of the closed-loop system, we propose to extend the widths of the interval parameters of the model (33). This extension is a compromise. In fact, if the widths of these interval parameters are too large, it is difficult to find a controller that respects both the stability and performances of the closed-loop. After some trials of controller design, we choose to expand the width of each interval parameter of (33) by 10%. It represents a good compromise between the extension of the width and the possibility to find a robust controller. Finally, the extended parameters of the interval model which will be used to compute the controller are:

$$\begin{aligned} [b_2] &= [6.937, 8.134] \times 10^{-8} \\ [b_1] &= [1.8067, 1.809] \times 10^{-4} \\ [a_2] &= [8.698, 9.898] \times 10^{-8} \\ [a_1] &= [5.227, 5.376] \times 10^{-6} \\ [a_0] &= [1.274, 1.456] \end{aligned} \quad (34)$$

4.4. Performances specifications

Microassembly and micromanipulation tasks generally require a submicrometric accuracy and high repeatability. Furthermore, the behavior of actuators used in these tasks is often desired to be without overshoot to ensure better quality tasks and to avoid destroying the manipulated micro-object or conversely to avoid the destruction of the actuators themselves. For all that, we consider the following specifications:

- behavior without or with small overshoot,
- settling time $tr_{5\%} < 30ms$,
- static error allowed $|\varepsilon| \leq 1\%$.

4.5. Computation of the closed-loop transfer

From the model $[G](s, [a], [b])$ in (33) and from the RST controller in (20) to be designed, we derive the closed-loop $[H_{cl}](s, [a], [b], [\theta])$:

$$[H_{cl}](s, [a], [b], [\theta]) = \frac{([t_1]s + 1)([b_2]s^2 + [b_1]s + 1)}{([s_1]s + [s_0])([a_2]s^2 + [a_1]s + 1) + ([r_1]s + [r_0])([b_2]s^2 + [b_1]s + 1)} \quad (35)$$

After developing (35), the closed-loop can be written as follows:

$$[H_{cl}](s, [p], [q]) = \frac{[q_3]s^3 + [q_2]s^2 + [q_1]s + 1}{[p_3]s^3 + [p_2]s^2 + [p_1]s + [p_0]} \quad (36)$$

where the boxes $[q]$, $[p]$ depend on the boxes $[a]$ and $[b]$ of the interval model and on the interval parameters $[\theta] = [[t_1], [r_0], [r_1], [s_1], [s_0]]$ of the controller as described below:

$$\begin{aligned} [q_3] &= [t_1][b_2] \\ [q_2] &= [t_1][b_1] + [b_2] \\ [q_1] &= [t_1] + [b_1] \\ [p_3] &= [s_1][a_2] + [r_1][b_2] \\ [p_2] &= [s_1][a_1] + [s_0][a_2] + [r_1][b_1] + [r_0][b_2] \\ [p_1] &= [s_1][a_0] + [s_0][a_1] + [r_0][b_1] + [r_1] \\ [p_0] &= [s_0][a_0] + [r_0] \end{aligned} \quad (37)$$

4.6. Computation of the interval reference model

The specifications in Section 4.4 can be transcribed into an interval reference model. According to the remark in Section 3.2, this reference model must have the same structure than the closed-loop (36). So, the reference model must have characterized by an order $n = m = 2$. We have:

$$[H](s) = \frac{(1 + \frac{[\tau]}{\kappa}s)^3}{\frac{1}{[K_e]} \cdot (1 + [\tau]s)(1 + \frac{[\tau]}{\kappa}s)^2} \quad (38)$$

Such as $[\tau] = [0, 10ms]$, $[K_e] = [0.99, 1.01]$ and $\kappa = 10$.

After developping (38), we obtain:

$$[H](s) = \frac{[x_3]s^3 + [x_2]s^2 + [x_1]s + 1}{[w_3]s^3 + [w_2]s^2 + [w_1]s + [w_0]} \quad (39)$$

Where the boxes $[x]$ and $[w]$ are function of the box $[[K_e], [\tau], [\kappa]]$ as follows:

$$\begin{aligned} [x_3] &= \frac{\tau^3}{\kappa^3} \\ [x_2] &= \frac{3\tau^2}{\kappa^2} \\ [x_1] &= \frac{3\tau}{\kappa} \\ [w_3] &= \frac{\tau^3}{\kappa^2 K_e} \\ [w_2] &= \frac{(1 + 2\kappa)\tau^2}{\kappa^2 K_e} \\ [w_1] &= \frac{(\kappa + 2)\tau}{\kappa K_e} \\ [w_0] &= \frac{1}{K_e} \end{aligned} \quad (40)$$

4.7. Derivation of the controller

The derivation of the controller consists to find the set (or subset) of the interval parameters $[\theta] = [[t_1], [r_0], [r_1], [s_1], [s_0]]$ for which specifications hold, i.e. find $[\Theta]$ such as:

$$\Theta := \left\{ \theta \in [\theta] \mid \begin{array}{l} [q_j](\theta) \subseteq [x_j], \forall j = 1, \dots, 3 \\ [p_i](\theta) \subseteq [w_i], \forall i = 0, \dots, 3 \end{array} \right\} \quad (41)$$

where $[[p_i], [q_j]]$ and $[[w_i], [x_j]]$ (for $i = 0 \dots 3$ and $j = 1 \dots 3$) are defined in (37) and (40) respectively.

Remark IV.1 *The number of unknown parameters (see (20)) are 5 while the number of inclusions (41) is 7. Therefore, there are more inclusions than unknown variables. In such situation, the set solution Θ is given by the intersection of the set solution of each inclusion in (41), i.e.:*

$$\Theta = \bigcap_{i=1}^7 (\text{set_sol})_i$$

such as: $(\text{set_sol})_i$ is the set solution of the i^{th} inclusion.

SIVIA algorithm is applied to solve the problem (41) and to characterize the set solution Θ . However, the computation time increases exponentially with the number of the parameters making difficult to solve such problem with multiple parameters. Since our objective is not to compute all possible controllers *RST* that ensure specifications but to find a set (or subset) of controllers *RST* satisfying desired behaviors of the

closed-loop (see Section 4.4), we choose to solve the problem (41) not through SIVIA alone but also through some hand-tuning prior this algorithm. The procedure consists to manually settle some parameters (as given scalars or as given intervals) and then to seek for the remaining parameters thanks to SIVIA.

The three first inclusions $[q_j] \subseteq [x_j]$ for $j = 1..3$ depend only on the parameter $[t_1]$, so they can be solved independently. These inclusions are linear and with one parameter which can be solved using SIVIA algorithm. After Application of SIVIA, we obtain the following solution:

$$[t_1] = [0, 2.81 \times 10^{-3}] \quad (42)$$

Now, it remains to solve the second part of the inclusions (41), i.e. the inclusions $[p_i] \subseteq [w_i]$ for $i = 0, \dots, 3$. In order to cancel the static error, i.e. $[p_0] = p_0 = 1$, the parameters $[s_0]$ and $[r_0]$ are manually adjusted as follows:

$$\begin{cases} [s_0] = s_0 = 0 \\ [r_0] = r_0 = 1 \end{cases} \quad (43)$$

which also confirms that the last inclusion $[p_0] \subseteq [w_0]$ is respected.

Finally, we have to solve the following problem with two parameters $[s_1]$ and $[r_1]$:

$$\begin{aligned} [s_1][a_2] + [r_1][b_2] &\subseteq \frac{\tau^3}{\kappa^2 K_e} \\ [s_1][a_1] + [r_1][b_1] + [b_2] &\subseteq \frac{1 + 2\kappa}{\kappa^2} \frac{\tau^2}{K_e} \\ [s_1][a_0] + [b_1] + [r_1] &\subseteq \frac{\kappa + 2}{\kappa} \frac{\tau}{K_e} \end{aligned} \quad (44)$$

To characterize the set solution $S_{s_1 r_1}$ of the parameters $[s_1]$ and $[r_1]$, we apply SIVIA algorithm for the second time to the inclusions (44). We choose an initial box $[s_{10}] \times [r_{10}] = [0.01 \times 10^{-3}, 10 \times 10^{-3}] \times [0.01 \times 10^{-3}, 10 \times 10^{-3}]$ and an accuracy of $\epsilon = 0.1 \times 10^{-3}$. The obtained subpaving is given in Fig. 5.

The area in blue corresponds to the inner subpaving $\underline{S}_{s_1 r_1}$ i.e. the set solution $[s_1] \times [r_1]$ of the inclusions (44). The area in white corresponds to the outer subpaving $\bar{S}_{s_1 r_1}$, it contains the boxes for which no decision on the test of inclusion in (44) can be taken. $\bar{S}_{s_1 r_1}$ can be minimized by increasing the computation accuracy. The boxes in red correspond

to the parameters $[s_1]$ and $[r_1]$ for which the inclusions (44) do not hold. A controller with the parameters $t_1 \in [0, 2.8 \times 10^{-3}]$, $s_0 = 0$, $r_0 = 1$ and any choice of s_1 , r_1 in the blue colored area $\underline{S}_{s_1 r_1}$ applied to the interval model (uncertain model) $[G](s, [a], [b])$ with parameters given in (34) will satisfy the required performances specified in Section 4.4.

Note that the set $\underline{S}_{s_1 r_1}$ does not represent the set of all possible controllers that satisfy the required performances but a subset of these controllers. Therefore, any change on the values of the parameters $[s_0]$ and $[r_0]$ leads to a change on the subset $\underline{S}_{s_1 r_1}$.

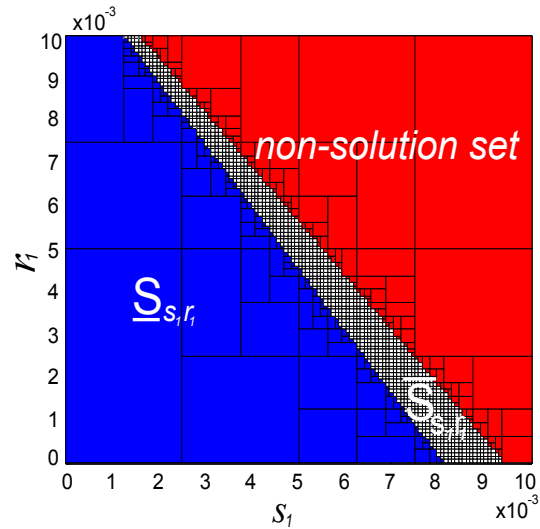


Fig. 5. Resulting subpaving $[s_1] \times [r_1]$

The searched inner subpaving $\underline{\Theta}$ is defined as follows:

$$\underline{\Theta} := \left\{ \begin{array}{l} \theta \in [\theta] | t_1 \in [0, 2.8 \times 10^{-3}], \\ r_1 = 1, s_0 = 0, \{s_1, r_1\} \in \underline{S}_{s_1 r_1} \end{array} \right\} \quad (45)$$

For the implementation, we choose the following polynomials for the RST controller:

$$\begin{aligned} R(s) &= 0.5 \times 10^{-3} s + 1 \\ S(s) &= 5 \times 10^{-3} s \\ T(s) &= 1 \times 10^{-5} s + 1 \end{aligned} \quad (46)$$

In fact, there is no method to choose the optimal controller that will ensure the best

behaviours of the closed-loop among these solutions $\underline{S}_{s_1 r_1}$. However, it is guaranteed that any choice inside them will ensure the specified performances.

V. Controller implementation and experimental results

5.1. Controller implementation

This part consists to apply the RST controller (46) to control the deflection of the piezocantilevers. For that, the closed-loop scheme in Fig. 1 is transformed into the scheme presented in Fig. 6 in order to have a causal controller:

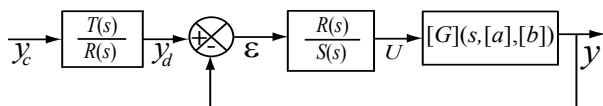


Fig. 6. Loop control with RST.

5.2. Experimental result

Fig. 7 presents the experimental results when a step reference input $y_c = 20\mu m$ is applied. As shown on Fig. 7, the computed controller has played its role. Indeed the experimental behavior of the closed-loop (tested on the two piezocantilevers) is without overshoot, with settling times $tr_1 = 19.5ms \leq 30ms$, $tr_2 = 21.5ms \leq 30ms$ respectively for the piezocantilevers 1 and 2 and the static errors remain bounded by the specified interval.

VI. Closed-loop stability analysis

In this section, we present a robust stability result of the closed-loop with the designed RST controller (Fig. 6). The stability analysis is done analytically and graphically. As the transfer $\frac{T(s)}{R(s)}$ is stable, the robust stability analysis of the closed-loop $\frac{y(s)}{y_c(s)}$ can be reduced to the robust stability analysis of the transfer $\frac{y(s)}{y_d(s)}$ (Fig. 6).

The stability analysis of an interval system is based on the roots of the corresponding characteristic polynomial. This polynomial is the denominator of the interval closed-loop system. The interval closed-loop system is stable if and only if

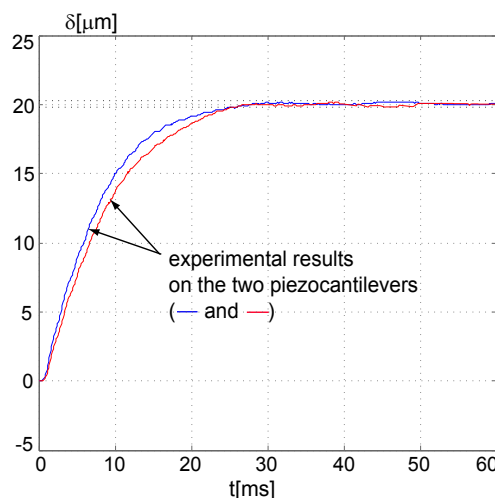


Fig. 7. Step responses envelope compared with the experimental results.

all the roots of the characteristic polynomial are in the left part \mathbb{C}^- of the complex plane.

The characteristic polynomial of the transfert from the input signal y_d to the output y is defined as follows :

$$[P](s) = [p_3]s^3 + [p_2]s^2 + [p_1]s + 1 \quad (47)$$

Such as: $[p_3] = [a_2]s_1 + [b_2]r_1$, $[p_2] = [b_2] + [a_1]s_1 + r_1[b_1]$, $[p_1] = [b_1] + r_1 + [a_0]s_1$.

where $r_1 = 0.5 \times 10^{-3}$ and $s_1 = 5 \times 10^{-3}$ are the parameters of the implemented polynomials $R(s)$ and $S(s)$ (46).

According to the Routh's criterion, all the roots of the interval polynomial $[P](s)$ are in the left part \mathbb{C}^- if and only if the following conditions are satisfied:

$$\begin{aligned} [p_3] &> 0 \\ [p_2] &> 0 \\ [p_1] &> 0 \\ [p_2][p_1] - [p_3] &> 0 \end{aligned} \quad (48)$$

After computation, we obtain:

$$\begin{aligned} [p_3] &= [4.696, 5.355] \times 10^{-10} > 0 \\ [p_2] &= [1.597, 1.7418] \times 10^{-7} > 0 \\ [p_1] &= [7.054, 7.962] \times 10^{-3} > 0 \\ [p_2][p_1] - [p_3] &= [5.951, 8.981] \times 10^{-10} > 0 \end{aligned} \quad (49)$$

As all the terms in (49) are strictly positive, the implemented controller ensure the robust stability for the interval system $[G](s, [a], [b])$.

Now let us analyze the δ -stability of the closed-loop. The δ -stability is an interesting information to evaluate a stability margin of a system. For that, instead of using the Laplace variable s , the variable $s - \delta$ (with $\delta > 0$) is used. So, the interval polynomial $[P](s)$ is δ -stable if and only if all its roots are in the part Γ_δ of the complex plane and located on the left of the vertical line $Re(s) = -\delta$. In this analysis, we compute the maximal δ for which the implemented RST controller still ensures the δ -stability for the interval system $[G](s, [a], [b])$. We can rewrite $[P](s - \delta)$ as follows:

$$[P](s - \delta) = \alpha_3 s^3 + \alpha_2 s^2 + \alpha_1 s + \alpha_0 \quad (50)$$

where:

$$\begin{aligned} \alpha_3 &= [p_3], & \alpha_2 &= [p_2] - 3\delta[p_3], & \alpha_1 &= [p_1] - \\ & 2\delta[p_2] - 3\delta^2[p_3] & \text{and} & & \alpha_0 &= 1 - \delta[p_1] + \delta^2[p_2] + \\ & 3\delta^3[p_3]. \end{aligned}$$

The polynomial $[P](s - \delta)$ is stable if and only if:

$$\begin{aligned} [\alpha_3] &> 0 \\ [\alpha_2] &> 0 \\ [\alpha_1] &> 0 \\ [\alpha_2][\alpha_1] - [\alpha_3][\alpha_0] &> 0 \end{aligned} \quad (51)$$

The resolution of this nonlinear inequalities problem leads to the admissible values of δ that satisfy the inequalities (51). After computation, we obtain the interval parameter δ :

$$\delta = [0, 30.493] \quad (52)$$

To resume, we can conclude that the implemented RST controller ensures the δ -stability for the interval system whatever δ less than 30.493.

Finally, we analyze the Black-Nichols diagram of the open-loop system $[L](s)$ in order to assess the stability margins (phase and gain). The open-loop $[L](s)$ is defined by:

$$[L](s) = \frac{R(s)}{S(s)} [G](s, [a], [b]) \quad (53)$$

Fig. 8 presents the Black-Nichols diagram of the open-loop system $[L](s)$ and that of the controlled system $[G](s, [a], [b])$. The Black-Nichols diagram of the interval system $[L](s)$ (resp.

$[G](s, [a], [b])$) encloses the Black-Nichols diagram of all the transfer functions contained in $[L](s)$ (resp. in $[G](s, [a], [b])$). From the figure, we can see first that the performances of the closed loop are improved relative to those of the system it-self. Indeed, the gain of $[L]$ tends towards ∞ when $w \rightarrow 0$ while that of $[G]$ is finite. This means that the static gain of the closed-loop tends towards zero, which is not the case for the non-controlled system $[G]$. This figure indicates also that the phase and the gain margins were improved when implementing the RST controller. They can be computed from the Black-Nichols diagram. For the controlled system, these margins are $M_\varphi \approx 95$ (at a pulsation about 150Hz) and $MG = \infty$ respectively.

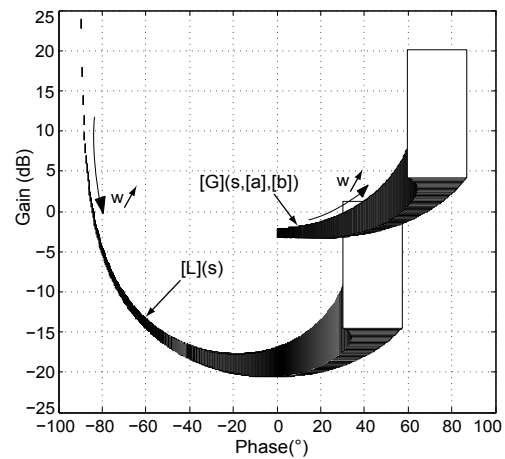


Fig. 8. Black-Nichols diagrams of the open-loop system $[L](s)$ and the interval system $[G](s, [a], [b])$.

VII. Conclusion

In this paper, a method to design robust controllers for systems with uncertain parameters has been proposed. While the uncertain parameters are described by intervals, the controller structure is given *a priori* (a fixed-order RST controller). The main advantages of the proposed approach are the natural way to model the uncertainties and the derivation of a low order controller. Starting from specified performances, the calculation of the controller parameters is formulated as a set-inversion problem that can be solved using an existing algorithm. Experimental tests of the proposed method were carried out on piezoelectric

actuators. The experimental results showed its efficiency. Finally, a stability analysis of the closed-loop was carried out and confirmed the robustness of the computed controller.

REFERENCES

- Barmish B R. 1994. *'New Tools for Robustness of Linear Systems'*, Macmillan, New York, USA.
- Dasgupta S, Anderson B D O., Chockalingam G, Fu M. 1994. *'Lyapunov functions for uncertain systems with applications to the stability of time varying systems'*, IEEE Trans. on Circuits and Systems, vol.41, pp.93-106.
- Jaulin L, Kieffer M, Didrit O, Walter E. 2001. *'Applied Interval Analysis'*, Springer.
- Bondia J, Kieffer M, Walter E, Monreal J, Picò J. 2004. *'Guaranteed tuning of PID controllers for parametric uncertain systems'*, IEEE CDC, 2948-2953.
- Dullerud G E, Paganini F G. 2000. *'A course in robust control theory: a convex approach'*, 1st edition, Springer.
- Reza Moheimani S O. 2001. *'Perspectives in Robust Control'*, 1st edition, Springer.
- Ur Rehman O, Fidan B, Petersen I. 2011. *'Uncertainty modeling and robust minimax LQR control of multivariable nonlinear systems with application to hypersonic flight'*, Asian Journal of Control, DOI: 10.1002/asjc.399.
- Sadeghzadeh A. 2011. *'Identification and robust control for systems with ellipsoidal parametric uncertainty by convex optimization'*, Asian Journal of Control, DOI: 10.1002/asjc.437.
- Chen W, Zhang Z. 2011. *'Nonlinear adaptive learning control for unknown time-varying parameters and unknown time-varying delays'*, Asian Journal of Control, DOI: 10.1002/asjc.403.
- Liu Y J, Tong S C, Li T S. 2010. *'Adaptive fuzzy controller design with observer for a class of uncertain nonlinear MIMO systems'*, Asian Journal of Control, DOI: 10.1002/asjc.214.
- Banjerdpongchai D, How J P. 1997. *'LMI Synthesis of Parametric Robust H_∞ Controllers'*, In Proceeding of the American Control Conference, pp.493-498.
- Balas G J, Doyle J C, Glover K, Packard A, Smith R. 1993. *' μ -Analysis and Synthesis Toolbox'*, The Mathworks Inc.
- Moore R E. 1966. *'Interval analysis'*, Prentice-Hall, Englewood Cliffs N. J.
- Kharitonov V L. 1978. *'Asymptotic stability of an equilibrium position of a family of systems of linear differential equations'*. Differential'nye Uravneniya, 14, 2086-2088.
- Walter E, Jaulin L. 1994. *'Guaranteed characterization of stability domains via set inversion'*, IEEE Trans. on Autom. Control, 39(4), 886-889.
- Wang C. 2010. *'New delay-dependent stability criteria for descriptor systems with interval time delay'*, Asian Journal of Control, DOI: 10.1002/asjc.287.
- Smagina Y, Brewerb I. 2002. *'Using interval arithmetic for robust state feedback design'*, Systems and Control Letters, 187-194.
- Chen C T, Wang M. D. 1997. *'Robust controller design for interval process systems'*. Computers & Chemical Engineering, 21, 739-750.
- Rakotondrabe M, 2011. *'Performances inclusion for stable interval systems'*, IEEE - ACC (American Control Conference), pp.4367-4372, San Francisco CA USA, June-July 2011.
- Li K, Zhang Y. 2009. *'Interval Model Control of Consumable Double-Electrode Gas Metal Arc Welding Process'*, IEEE - Trans. on Automation Science and Engineering (T-ASE), 1-14.
- Chen C T, Wang M D. 2000. *'A two-degrees-of-freedom design methodology for interval process systems'*, Computers and Chemical Engineering, 23, 1745-1751.
- Bondia J, Picò J. 2003. *'A geometric approach to robust performance of parametric uncertain systems'*, International Journal of Robust and Nonlinear Control, vol. 13, 1271-1283.
- Khadraoui S, Rakotondrabe M, Lutz P. 2010. *'Robust control for a class of interval model: application to the force control of piezoelectric cantilevers'*, IEEE - CDC, pp.4257-4262, Atlanta Georgia USA.
- Jaulin L, Walter E. 1993. *'Set inversion via interval analysis for nonlinear bounded-error estimation'*, Automatica, 29(4), 1053-1064.
- Bargiel S, Rabenoroso K, Cleve C, Gorecki C, Lutz P. 2010. *'Towards Micro-Assembly of Hybrid MOEMS Components on Reconfigurable Silicon Free-Space Micro-Optical Bench'*, Journal of Micromechanics and Microeng., 20(4).
- Haddab Y, Chaillet N, and Bourjault A. 2000. *'A microgripper using smart piezoelectric actuators'*, IEEE/RSJ International Conference on Intelligent Robot and Systems (IROS), Takamatsu - Japan, 1, 659-664.
- Agnus J, Breguet J M, Chaillet N, Cois O, De Lit P, Ferreira A, Melchior P, Pellet C,

- Sabatier J. 2003. *'A smart microrobot on chip: design, identification and modeling'*, IEEE/ASME AIM, Kobe Japan, 685-690.
28. M. Rakotondrabe, Y. Haddab and P. Lutz, 'Quadrilateral modelling and robust control of a nonlinear piezoelectric cantilever', IEEE - Trans. on Control Systems Technology, 17(3), pp:528-539, May 2009.
29. Yi-Chen Huang and De-Yao Lin, 'Ultra-fine tracking control on piezoelectric actuated motion stage using piezoelectric hysteretic model', Asian Journal of Control, 6(2), p.208-216, 2004.
30. J-C. Shen, W-Y. Jywe, C-H. Liu, Y-T. Jian and J. Yang, 'Sliding-mode control of a three-degrees-of-freedom nanopositioner', Asian Journal of Control, 10(3), p.267-276, 2008.